Optimal Allocation Research of Distribution Network with DGs and SCs by Improved Sand Cat Swarm Optimization Algorithm

Hongyu Long, Yuqiang He, Yuansen Xu*, Chun You, Diyang Zeng and Hu Lu

***Abstract*—The contemporary paradigm for developing novel distribution grids is centered on the integration of distributed generations (DGs) and shunt capacitors (SCs) within the distribution infrastructure. Unreasonable DG and SC configurations may have a negative impact on grid line loss and voltage quality. The goal of optimal allocation research of distribution network (OARDN) is to allocate distributed generators (DGs) and shunt capacitors (SCs) in the distribution network in a rational manner to minimize power losses, enhance voltage quality, and ensure secure and stable power supply to the loads. Aiming at the critical OARDN problems, such as minimizing power loss and improving voltage quality, this paper proposes an improved sand cat swarm optimization algorithm (ISCSO). To address the issue of the original SCSO being prone to local optima and low search accuracy, this method introduces a tent map-based chaotic strategy and reverse learning approach to augment the precision of the optimization, and proposes a cross-learning mechanism to expand the global search ability, and this method is used to solve the single-objective problem. Based on ISCSO, the sensitivity analysis method and pareto non-inferior sorting method are introduced, which is extended to the MOISCSO algorithm to solve multi-objective OARDN problem.**

Simulation experimental results on IEEE33, IEEE69, and IEEE119 test systems and comparison with other scholars' research results show that the proposed method is practical and competitive for solving single-objective and multi-objective OARDN problems.

***Index Terms*—tent map-based chaotic strategy, reverse learning approach, cross-learning mechanism, sensitivity analysis method**

Manuscript received January 12, 2023; revised March 27, 2023.

Hongyu Long is a professor level senior engineer at Chongqing Key Laboratory of Complex Systems and Bionic Control, Chongqing University of Posts and Telecommunications, Chongqing 400065, China (e-mail: longhongyu20@163.com).

Yuqiang He is a postgraduate student at Chongqing Key Laboratory of Complex Systems and Bionic Control, Chongqing University of Posts and Telecommunications, Chongqing 400065, China (e-mail: heyuqiang_cq@163.com).

Yuansen Xu is a senior engineer at the Economic and Technology Research Institute of State Grid Chongqing Electric Power Company, Chongqing 401120, China (corresponding author to provide phone: +8613996108500; e-mail: xuyuansen_cq@163.com).

Chun You is a senior engineer at the Economic and Technology Research Institute of Stat24e Grid Chongqing Electric Power Company, Chongqing 401120, China (e-mail: youchun_cq@163.com).

Diyang Zeng is a professor at the School of Electric Power Engineering, Nanjing Institute of Technology, Nanjing 211167, China (e-mail: zengdiyang_nj@163.com).

Hu Lu is a senior engineer at the Chongqing Jiangbeizui Water Air Conditioning Co., Ltd., Chongqing 404100, China (e-mail: luhu_cq@163.com).

I. Introduction

DISTRIBUTION network is the last link in power transmission grid, and the quality of its power transmission is the most important concern for electricity consumers [1]. In conventional distribution network, the electrical energy is mainly provided by the main substation at the beginning, and the voltage will fall along the power transmission direction thus resulting in a voltage lower than the rated voltage at the terminal, in addition, during transmission, the power losses in the system are very high, sometimes reaching about 30% of the load of the entire distribution system due to the excessive length of the transmission lines and the aging of the equipment [2], which further adversely affects the voltage distribution in the system [3], and this is a major challenge for the grid operator. Many scholars have found that the power loss is caused by reactive power, and try to deploy shunt capacitors (SCs) to reduce the power loss. SC has been widely used in radial distribution system because of its lower operating cost, lower loss and simple maintenance [4-6].

In recent years, a new distribution network has been established under the extensive research of renewable energy and the large-scale application of distributed generation. The introduction of distributed generators (DGs) in the distribution network results in a shift from unidirectional power flow to bidirectional power flow, which effectively reduces the power loss of the entire system and leads to a significant improvement in voltage quality [7-10]. Therefore, it is a current trend to combine DG and SC to optimize the power flow of distribution network [11]. However, reasonable DGs and SCs configurations have positive effects on the distribution network. In contrast, unreasonable configurations may not be beneficial to the distribution network and even have a noticeable impact on the distribution network [12,13]. Therefore, it is very essential to determine the location and capacity of DGs and SCs to minimize power loss and improve the voltage quality, which makes the OARDN problem a very interesting and hot research topic in recent years [14].

OARDN problem is a nonlinear and constrained optimization problem, for such an optimization problem, previous research methods often relied heavily on mathematical approaches for problem-solving [15-17], but the traditional methods to solve such problems have strong limitations, while the population intelligence optimization algorithms derived in recent years can solve the OARDN problem well, such as the discrete artificial bee colony algorithm [18], DE algorithm [19,20], HPSO algorithm [21], and hyper-cube ant colony algorithm [22], and many scholars have given solutions. Srinivas Nagaballi has studied the problem by using strategy with game theory for the optimal allocation of distributed power sources in railroad systems [23]. Truong proposes the QOCSOS algorithm with a chaotic local search strategy to optimize the allocation of distributed power sources [24]. Mikail Purlu and Belgin Emre Turkay et al. used heuristics to minimize annual energy loss and voltage deviation indexes for the optimal configuration of renewable distributed power sources [25]. Armin Arasteh applied IWOA to find the best spots and sizes for distributed generation units [26]. M. R. ELKADEEM proposed a novel approach to improve the HHO algorithm for solving the OARDN problem [27]. T. S. Tawfeek proposed the analytical algorithm and PSO algorithm and used these two algorithms for tidal analysis of distribution networks [28]. Most of the above literature mainly solved the single-objective OARDN challenge. For the multi-objective OARDN challenge, many scholars used the weighting coefficient method to accumulate multiple objective values, and such a method has strong subjectivity and limitation, and it is difficult to determine a reasonable weighting coefficient [29,30]. In the traditional OARDN research, most scholars prefer to study the optimization effect of different configurations of DG on optimization objective function. While the joint configuration of DG and SC is seldom studied. At the same time, many scholars ignore the influence of the power factor of DG on the optimization results. For this reason, this paper investigates the number and location of DG and SC and the setting of power factor.

On this basis, the improved sand cat swarm optimization algorithms (ISCSO and MOISCSO) are proposed in this paper and applied to the OARDN problem for the first time. For the OARDN problem with nonlinear and multiple constraints, two different constraint processing strategies are proposed to adapt the single-objective and multi-objective optimization issues, respectively. Simulation experiments are performed on three different test systems, namely IEEE33, IEEE69, and IEEE119, to confirm the efficacy of the proposed approach. The results are then compared to those of other researchers. The simulation outcomes demonstrate that the proposed method offers significant advantages in solving the OARDG problem with DGs and SCs, which leads to enhanced safety and stability of the distribution network.

The remainder of the paper is organized as follows: Section II presents the mathematical model of OARDN. Section III shows the improved methods of ISCSO and MOISCSO. Section IV shows the application of the proposed methods to single-objective and multi-objective OARDN problems with DG and SC, and Section V provides a comprehensive conclusion.

II. Problem Formulation

Essentially, the OARDN problem is a nonlinear multi-constraint optimization problem with complex engineering application background. This study achieves the optimal sizing and placement of DGs and SCs in the distribution network, considering specific objectives and fulfilling all the constraints. Therefore, from the mathematical form, the OARDN problem consists of three parts: the optimization of the objective function, fulfillment of the constraints, and the techniques used to address these constraints.

A. Objective Functions

1) Minimum active power loss

The power in the distribution network comprises both longitudinal and transverse components of energy, given that the power factor is typically lower than 1. Whether it is power grid operators or power consumers, we are more concerned about the active power loss in the whole system [31]. Therefore, the first optimization function is to reduce the active losses in the system.

$$P_{loss,Li} = I_{Li}^2 \times R_{Li} \tag{1}$$

$$P_{loss} = \sum_{i=1}^{N_L} P_{loss,Li} \tag{2}$$

$$f_1 = \min(P_{loss}) \tag{3}$$

$P_{loss,Li}$ represents the active power loss of the ith branch, I_{Li} represents the current flowing through the ith branch, R_{Li} represents the total resistance on the ith branch, and N_L represents the total number of branches in the system, P_{loss} represents the sum of the active power losses of all branches, i.e., active component of grid losses. The objective function aims to reasonably allocate the location and size of the DGs and SCs connected to the distribution network to reduce the active network loss of the whole system.

2) Minimal voltage deviation

In power distribution systems, the evaluation criteria for electric energy include the quality of voltage. In the traditional distribution networks, power is always provided by the head end, and the voltage at the end nodes of the system is often lower than the rated voltage. When distributed power sources and reactive power compensators are connected to the distribution network, they have a positive impact on the system, but the unreasonable configuration of DGs and SCs can cause shocks to the system, making the voltage at some nodes exceed the rated voltage. Therefore, minimizing the total voltage deviation in the system is the second optimization objective that should be considered. Its mathematical form is reflected in equation (4):

$$CVd = \sum_{i=1}^{N_Q} (V_i - V_{ref})^2 \tag{4}$$

$$f_2 = \min(CVd) \tag{5}$$

In which, CVd denotes the voltage deviation, V_i denotes the voltage of the ith PQ node, and V_{ref} represents the reference voltage, with a unit value of 1 (p.u.). N_Q denotes the number of PQ nodes. The objective function aims to raise the voltage of all nodes to a rated voltage of about 1.0 (p.u.).

B. Constraints

All constraints must be met for all configurations of equipment aimed at solving the objective function. The constraints of OARDN include an equality part and an inequality part.

1) Equality Constraints

When optimizing the objective function in OARDN, it is necessary to ensure the power balance constraint is satisfied for both active and reactive power [32].

The equations are defined as follows:

$$P_S+\sum_{k=1}^{N_{DG}}P_{DG,k}=\sum_{j=1}^{N_n}P_{Load,j}+\sum_{i=1}^{N_L}P_{loss,Li} \tag{6}$$

$$Q_S+\sum_{k=1}^{N_{DG}}Q_{DG,k}+\sum_{m}^{N_{SC}}Q_{SC,m}=\sum_{j=1}^{N_n}Q_{Load,j}+\sum_{i=1}^{N_L}Q_{loss,Li} \tag{7}$$

Where P_S, Q_S denote the active and reactive power supplied by the substation, $P_{DG,k}$, $Q_{DG,k}$ denotes the two components of capacity output of the kth distributed generation (when the power factor of distributed generator is not 1). $Q_{SC,m}$ denotes longitudinal component of capacity injected by the mth SC equipment. $P_{Load,j}$ and $Q_{Load,j}$ denotes the components of capacity on the jth node. $P_{loss,Li}$ and $Q_{loss,Li}$ denotes the power losses on the ith branch. N_{DG} is the quantity of distributed generations, N_{SC} is the quantity of static reactive power compensators, and N_n denotes the quantity of nodes in the grid.

2) Inequality Constraints

The inequality constraints in this context can be further classified as either controlled or control variable expressions. Among them, node voltage and branch current belong to state variables, power factor and capacity size belong to control variables.

1: Node Voltage Constraint

In solving the objective function, the voltage measurement at each grid point must satisfy inequality (8); otherwise, the system will be damaged when the voltage deviates from the rated value.

$$V_{\min}\le V_i\le V_{\max}\ ,\ i\in 1,2,...,N_n \tag{8}$$

Where $V_{\min}$ and $V_{\max}$ represent the minimum and maximum allowable values of each node voltage.

2: Branch current constraint

To consider the issue of the carrying capacity of each line in the distribution network, the current flowing through each branch must be limited.

$$\left|I_i\right|\le I_{i,\max}\ \ ,\ i\in 1,2,...,N_L \tag{9}$$

3: Power Factor Constraint

$$pf_{min,k}^{DG}\le pf_k^{DG}\le pf_{max,k}^{DG} \tag{10}$$

Where pf_k represents the power factor of the kth distributed generation, pf_{max} and pf_{min} represent power factor limits of a single distributed generation, respectively. The power factor formula is:

$$pf_k^{DG}=\frac{P_{DG,k}}{\sqrt{\left(P_{DG,k}\right)^2+\left(Q_{DG,k}\right)^2}} \tag{11}$$

4: Capacity constraint of DGs and SCs

The capacity of the devices configured in the system should be limited to a certain range, and their total capacity must not surpass 80% of its rated capacity. The aim of this is to reduce the cost of operation and the security of the grid.

$$\sum_{k=1}^{N_{DG}}P_{DG,k}\le 0.8\times\sum_{j=1}^{N_n}P_{Load,j} \tag{12}$$

$$\sum_{k=1}^{N_{DG}}Q_{DG,k}+\sum_{m=1}^{N_{SC}}Q_{SC,m}\le 0.8\times\sum_{j=1}^{N_n}Q_{Load,j} \tag{13}$$

3) Constraint Processing Strategy

In previous studies, many scholars have used the penalty coefficient approach to deal with the constraints in the OARDG problem. This approach requires artificially setting penalty coefficients, which has a strong subjectivity. When the penalty coefficients are not selected properly, the results of the objective function will be affected. Therefore, this paper proposes two constraint processing strategies to devise solutions that cater to both the single-objective and multi-objective variants of the OARDN issue, respectively.

1: Single-objective constraint processing strategy

Upon performing the power flow calculation, the equality constraint of OARDN is deemed satisfied. The inequality constraint processing strategy is implemented as follows.

$$CX_k=\begin{cases}CX_{k,\min} & if\ \ CX_k<CX_{k,\min}\\ CX_k & if\ \ \mathrm{CX}_{k,\min}<CX_k<CX_{k,\max}\\ CX_{k,\max} & if\ \ CX_{k,\max}<CX_k\end{cases} \tag{14}$$

The specific execution process can be explained as follows: when the program performs the next loop, the control variable CX_k is updated for each solution, and in order to satisfy its limited range, when the value of CX_k is less than the value of its lower limit $CX_{k,min}$, then CX_k=$CX_{k,min}$ is made, and when the value of CX_k is higher than the value of its upper limit $CX_{k,max}$, then CX_k=$CX_{k,max}$ is made.

The state variable inequality constraints are processed as follows.

Step 1: Each solution corresponds to an objective function value f=$f(CX, SX)$ and a total violation value C_{vio}. CX denotes the control variable, and SX denotes the state variable. The total violation value is specifically calculated as follows.

$$C_{vio,i}=\begin{Bmatrix}SX_i-SX_{\max,i},\ \text{if}\ \ SX_i>SX_{\max,i}\\ SX_{\min,i}-SX_i,\ \text{if}\ \ SX_i<SX_{\min,i}\end{Bmatrix} \tag{15}$$

$$C_{vio}=\sum_{i=1}^{n}C_{vio,i} \tag{16}$$

Step 2: When any two solutions j and k, compare their total violation values $C_{vio}(j)$, $C_{vio}(k)$, and if the total violation of $C_{vio}(j) < C_{vio}(k)$, the jth solution is described as better than the kth solution. If the total violation values are equal, the objective function values are compared.

2: Multi-objective constraint processing strategy

Based on the single-objective constraint processing strategy step, when the total violation value $C_{vio}(j)$ is less than $C_{vio}(k)$, the solution j dominates the solution k. When the total violation values are the same, compare the target value of each solution. Specific execution process is as follows:

$$\begin{cases}\forall\ \ l\in\{1,2,...n\} & f_l(j)\le f_l(k)\\ \exists\ \ m\in\{1,2,...n\} & f_m(j)<f_m(k)\end{cases} \tag{17}$$

Where n denotes the quantity of target goals, and $f_l(j)$ denotes the lth target goal of solution j. When all the target goal values of solution j are smaller than solution k, and there is at least one target goal value in solution j that is smaller than solution k, the solution j is superior to solution k, also known as solution j dominates solution k.

Multi-objective optimization is to find the most suitable pareto optimal set (POS) to make the value of each objective function as small as possible. For this reason, the paper proposes a pareto non-inferior sorting method to filter out the POS, based on calculating the rank of each solution for the hierarchy and calculating the congestion degree of each solution for the sorting.

a) Rank

Each solution in the population is assigned two sets, namely $N(i)$ and $S(i)$. $N(i)$ is the number that administrate the i-th individual. Whereas $S(i)$ denotes the number of individuals occupied by individual i. The next phase involves identifying every solutions in group that satisfy $N(i)$=0 and storing them in the set $F(1)$. The quantity of solutions in $F(1)$

is recorded as M, and their rank is assigned the value of $Rank_{(0)}$, which is assigned to 1. For solution l, the pool of solutions administrated by l (i.e., $S(l)$) is identified, then 1 is subtracted from $N(l)$ for each solution l in the set $S(l)$. This process is repeated for all solutions until their respective ranks have been determined and they have been allocated to the appropriate set, $F(i)$.

b) Congestion degree

The solution with a lower hierarchy is preferred when the solutions are at different hierarchies. When they are in the same hierarchy, they are sorted by calculating the congestion degree, and the solutions with a higher congestion degree are selected first. The following formula utilized for evaluating the congestion degree:

$$CD_l(i) = \frac{f_l(i+1) - f_l(i-1)}{f_{l,\max} - f_{l,\min}} \tag{18}$$

$$CD(i) = \sum_{l=1}^{N} CD_l(i) \tag{19}$$

Where, $CD(i)$ denotes the congestion degree of solution i. N denotes the number of objective functions. $f_{l,min}$ and $f_{l,max}$ denote the lower and upper bounds, respectively, of the l-th target goal.

III. Improvement of SCSO Algorithm

A. Original SCSO Algorithm

The sand Cat Swarm Optimization (SCSO) algorithm is a novel swarm intelligence optimization algorithm. It was proposed by Amir Seyyedabbasi and Farzad Kiani in 2022 [33], inspired by the fact that sand cats in nature have incredible hunting ability as well as low-frequency detection ability. The algorithm has been validated on two versions of the benchmark function test set, CEC14 and CEC15, and the results demonstrate this approach possesses superior capability compared to other swarm intelligence optimization methods. The search process of SCSO is similar to other swarm intelligence optimization algorithms, the search process of the SCSO algorithm can be divided into two phases, a local search phase and a global search phase. An obvious advantage of this approach is that there are few parameter settings and a very balanced conversion process between global and local search.

The process of optimizing the SCSO algorithm is outlined below: according to the size of the problem and the number of self-defined populations to generate the initialized population matrix, set the expression of each solution as $X_i=(X_{i,1}, X_{i,2},\ldots X_{i,j})$. The SCSO algorithm is inspired by the auditory abilities of sand cats at low frequencies, and its mathematical model can be represented by formula (20).

$$L_G = LSC - \left(\frac{2 \times LSC \times k}{2 \times k_{\max}}\right) \tag{20}$$

The acronym LSC stands for the auditory features of sand cats and is set to a value of 2. The variable k denotes the current iteration number, while k_{max} denotes the maximum allowed iteration number. During the initial search for the optimal algorithm, a global search process needs to be executed to perform a large-scale search, thus limiting the approximate range of solution. The specific execution formula is given in (21).

$$X_{i(k+1)} = r \times (X_{bs(k)} - rand \times X_{i(k)}) \tag{21}$$

$$r = LG \times rand \tag{22}$$

Where $X_{bs(k)}$ symbolizes the best solution at the kth loop, During the kth iteration, $X_{i(k)}$ serves as a symbol for the current solution, while $rand$ symbolizes a randomly generated number between 0 and 1. The local search process is then executed.

$$X_{i(k+1)} = X_{bs(k+1)} - X_{rnd} \times \cos(\theta) \times r \tag{23}$$

Where X_{rnd} represents a random solution. The SCSO algorithm's shift from overall exploration stage to partial exploration stage is regulated by the parameter R. When the magnitude of R exceeds 1, the global search phase is carried out, and vice versa for the local search phase. The expressions are as follows:

$$R = 2 \times LG \times rand - LG \tag{24}$$

B. Improved SCSO Algorithm

In solving the OARDN problem, the SCSO algorithm can not find the best optimal solution, and also the convergence accuracy is not high. The reason for this is that the algorithm's scope is too limited during the global search phase, making it incapable of escaping from local optimal solutions. Therefore, this paper proposes three improvement methods to enhance the comprehensive performance of the SCSO algorithm.

1) Tent map-based chaotic strategy

Tent map-based chaotic strategy has been introduced to widen the search space during the initial phase of the method, with the goal of avoiding the possibility of missing potential solutions.

$$X_{n+1} = f(x_n) = \begin{cases} x_n / a \ , x_n \in [0, a) \\ (1 - x_n)/(1-a) \ , x_n \in [a, 1] \end{cases} \tag{25}$$

The function is a chaotic mapping within its parameter range and has a uniform distribution function and good correlation. In the range of a, the system is in a chaotic state, and when a is 0.5, the system is in a short-period state.

2) Reverse learning approach

After expanding the initial search range of the algorithm, the optimal solution set will appear in this range. To reduce the search time of the algorithm while further approximating the optimal solution, the reverse learning approach will be introduced into the SCSO algorithm.

$$reverseX_{i,j} = X_{i,j(\max)} + X_{i,j(\min)} - X_{i,j} \tag{26}$$

The value of the control variable of solution i in the optimal configuration of the distribution network is represented by $X_{i,j}$, which denotes the initial position of solution i along the jth dimension. $reverseX_{i,j}$ represents the inverse solution corresponding to $X_{i,j}$.

3) Cross learning mechanism

To prevent the algorithm from getting stuck in local optima, lacking precision, and other shortcomings during the search phase, a cross-learning mechanism will be introduced.

$$\begin{gathered} X_{i,j(k+1)} = X_{r1,j(k)} + \eta \times (X_{r2,j(k)} - X_{r3,j(k)}) \\ r1、r2、r3 \in [1, N] \end{gathered} \tag{27}$$

Where $X_{i,j(k+1)}$ denotes a new solution generated after the cross-learning mechanism. $r1$, $r2$, and $r3$ are uniformly distributed random numbers in the interval [0, 1]. η is a step factor, which regulates the extent of cross-fusion and is assigned to 0.5. $X_{r1,j(k+1)}$, $X_{r2,j(k+1)}$, and $X_{r3,j(k+1)}$ denote three different solutions taken from the parent generation.

The pseudo-codes of the proposed ISCSO and MOISCSO algorithms to solve the single-objective and multi-objective OARDN problems are shown in TABLE I and TABLE II, the process diagrams are shown in Fig. 1 and Fig. 2.

TABLE I
PSEUDO-CODE OF ISCSO ON SINGLE-OBJECTIVE OARDN PROBLEM

Start
Step 1: Identify the data of the system and generate the initial population, using (25, 26)
Step 2: Compute the target goal value Pl_{oss}, CV_d and the violation value C_{vio} for all individuals.
Step 3: Record the optimal solution for both the group and individual.
Set the number of iterations $k=0$
while $k < k_{max}$
Update the value of L_G by (20);
if $\|R\|>1$
Update populations by (21);
else
Update populations by (23);
end
Implementation of Step 2 and Step 3
Compare the group optimum solution and the individual optimum solution for the kth and k-1th generations;
Update group optimal solution and individual optimal solution;
$k=k+1$;
end while

TABLE II
PSEUDO-CODE OF MOISCSO ON MULTI-OBJECTIVE OARDN PROBLEM

Start
Step 1: Identify the data of the system;
Step 2: Select the installation position of DG and SC according to the sensitivity degree analysis, generate the initial population, using (25, 26);
Step 3: Compute the objective function value Pl_{oss} and CV_d for all individuals, rank and sort all individuals and store them in an external file;
Set the number of iterations $k=0$
while $k < k_{max}$
Update the value of L_G by (20);
if $\|R\|>1$
Update populations by (21);
else
Update populations by (23);
end
Calculate the objective function value Pl_{oss} and CV_d for all individuals;
Merge current populations with populations in external files for ranking and sorting;
Update the populations in the external file and record the objective function value Pl_{oss} and CV_d for all individuals
$k=k+1$;
end while

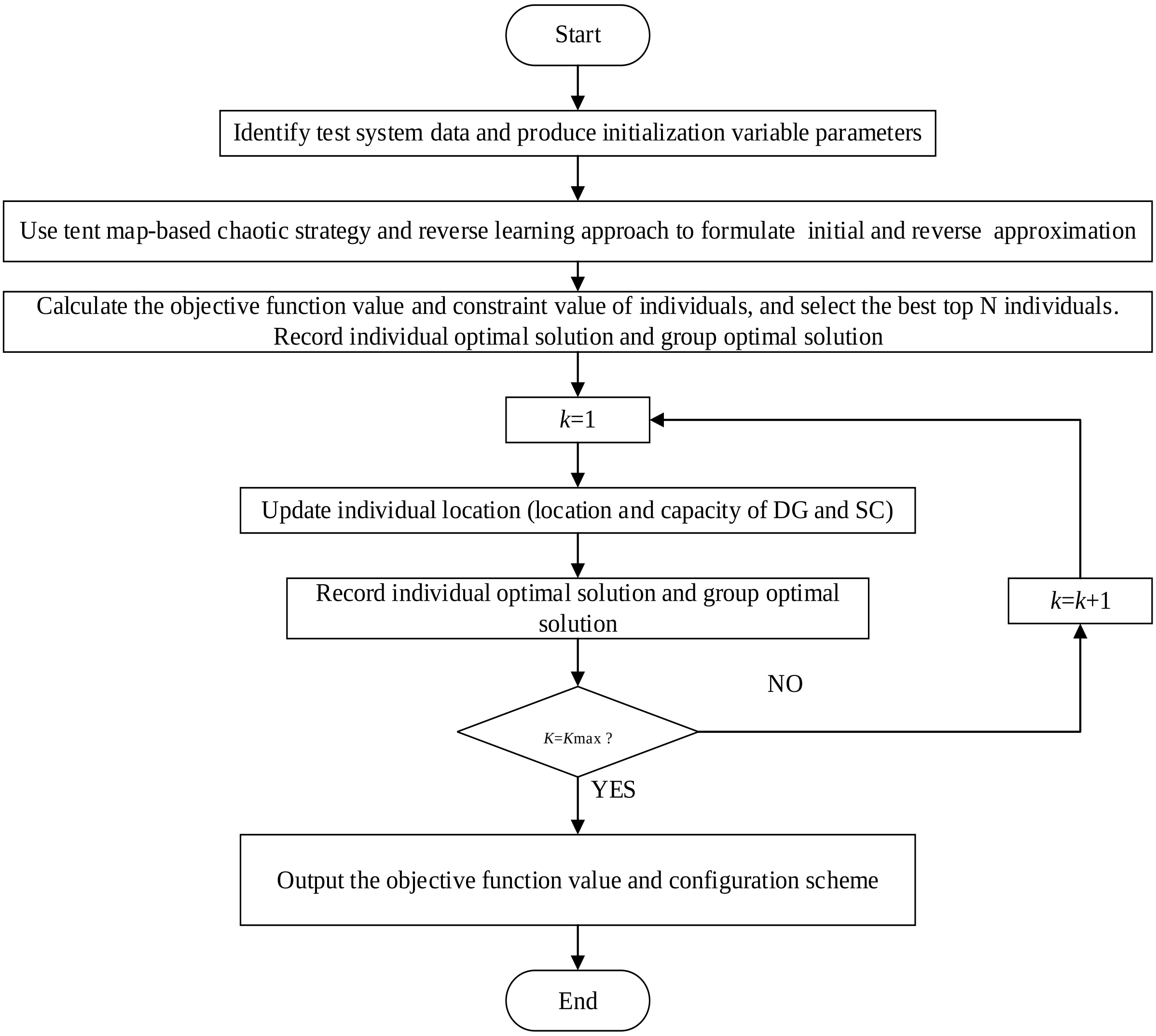

Fig. 1. The process diagram of single-objective OARDN problem

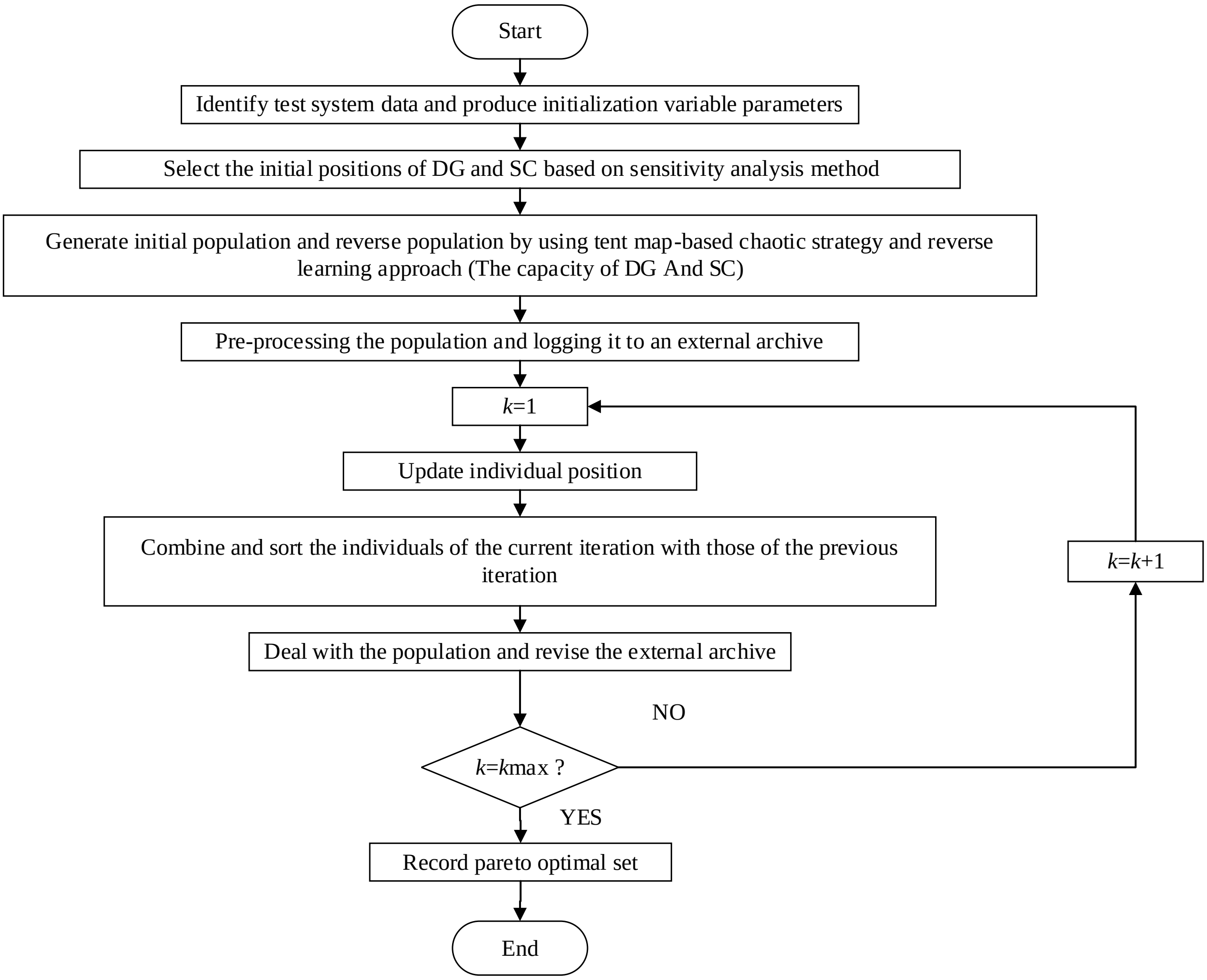

Fig. 2. The process diagram of Multi-objective OARDN problem

IV. SIMULATION EXPERIMENT AND COMPARISON

In response to the limitations of the SCSO, three improvements are introduced and enhanced algorithms, ISCSO and MOISCSO, are proposed for single and multi-objective applications. To assess the advancement and superiority of the method in detail, single and multi-objective experiments will be carried out on various combinations of DGs and SCs configurations across three different test systems.

Set the population size of the single-objective experiment to 30 and the number of iterations to 100. The multi-objective experiments are conducted with a population size of 100 and a maximum iteration limit of 300. Such parameter settings are enough for achieving the optimal solution within a minimal time, and it will not waste computer computing resources.

A. Single Objective Simulation for OARDN

1) Case1

In this case, the experiment of the single-objective OARDN problem will be conducted on IEEE33 test system. The ISCSO method is adopted to verify the deployment of 15 different combinations of DG and SC for minimizing power loss and voltage deviation in the system. There are two types of combinations of DG and SC: the first type is that the power factor of DG unit is 1, which includes three independent configurations of DG, three independent configurations of SC and three combinations of combined configurations of DG and SC; the second type is that the power factor of DG unit is 0.9, which includes three independent configurations of DG and three combined configurations of DG and SC.

TABLE III presents the optimization results for the first type of configuration scheme and the results compared with other studies. The table shows the detailed active power loss values P_{loss} and voltage deviation values CV_d for different configuration schemes.

By observing this table, it can be clearly seen that when a DG is deployed in the distribution network, the active power loss can decrease by nearly 50% compared with the active power loss generated by the original system, which reflects that the deployment of distributed generation has a positive effect on the stable operation of the distribution network, and further illustrates that it is necessary to study OARDN. With the increase of DG number, the active power loss will further decrease, from 111.03 KW to 77.36 KW. At the same time, it can be seen that the voltage deviation decreases from 0.0377 (p.u.) to 0.0171 (p.u.). However, the magnitude of the decrease is decreasing. This indicates that the rational allocation of distributed generation has a good improvement on both power loss and voltage stability of the distribution network. As the results of similar studies are shown in the

TABLE III
THE FIRST TYPE OF CONFIGURATION SCHEME AND COMPARISON RESULTS FOR CASE1 (PF=1)

Configuration	Algorithms	Capacity (Location) of DGs	Capacity (Location) of SCs	P_{loss} (KW)	Percentage of original P_{loss} reduction	CV_d (p.u.)
	Case33			212.83		0.1223
1DG	ISCSO	2590.23(6)	-	111.03	47.83%	0.0377
	BSOA [34]	1.8575(8)		118.1	44.51%	
2DG	ISCSO	851.15(13) 11580.01(30)	-	87.16	59.05%	0.01695
3DG	ISCSO	822.68(13) 407.47(25) 1086.59(30)	-	77.36	63.65%	0.0171
	ALO [35]	148.5(10) 520.8(13) 1360.8(30)	-	86.40	59.40%	-
	LSFSA [36]	1112.4(6) 487.4(18) 867.9(30)	-	82.03	61.46%	-
	GA-IWD [37]	1221.4(11) 683.3(16) 1213.5(32)	-	110.51	48.06%	-
1SC	ISCSO	-	1258.03(30)	151.38	28.87%	0.0838
2SC	ISCSO	-	524.87(11) 920.00(30)	142.45	33.07%	0.0650
3SC	ISCSO	-	454.65(12) 485.11(29) 613.33(30)	141.72	33.41%	0.0633
1DG+1SC	ISCSO	2531.59(6)	1256.00(30)	58.45	72.54%	0.0173
	WOA [38]	2557.6(6)	1762(6)	67.86	68.12%	
2DG+2SC	ISCSO	949.29(12) 1091.28(30)	503.01(11) 920.00(30)	29.02	86.36%	0.0019
	IMDE [39]	1080(10) 896.4(31)	254.8(16) 923.3(30)	32.08	84.97%	-
3SG+3SC	ISCSO	503.34(6) 730.39(14) 971.60(30)	613.17(6) 276.81(14) 612.54(30)	23.73	88.85%	0.0017
	GABC [40]	1098(28) 132(29) 609(30)	644.03(13) 602.81(24) 750(30)	93.72	55.96%	-

TABLE IV
The Second Type of Configuration Scheme for Case1 (PF=0.9)

Configuration	Algorithms	Capacity (Location) of DGs	Capacity (Location) of SCs	P_{loss} (KW)	Percentage of original P_{loss} reduction	CV_d (p.u.)
	Case33			212.83		0.1223
1DG	ISCSO	2766.19(6)	-	70.86	66.71%	0.0172
2DG	ISCSO	842.77(13) 1344.10(30)	-	35.24	83.48%	0.0019
3DG	ISCSO	753.79(14) 985.25(24) 1232.78(30)	-	18.58	91.27%	0.0012
1DG+1SC	ISCSO	2582.53(6)	400.60(31)	57.46	73%	0.0015
2DG+2SC	ISCSO	825.57(13) 1236.24(30)	200.30(7) 200.30(32)	28.53	86.59%	0.0014
3SG+3SC	ISCSO	769.02(13) 1002.20(24) 1200.02(30)	113.46(2) 120.89(3) 108.97(5)	16.93	92.05%	0.0012

table, it can be seen that the ISCSO algorithm proposed in this paper is more competitive and better optimized than the ALO, LSFSA, and GA-IWD algorithms for the configuration of three DGs.

When the combination of three independently configured SCs is deployed in the system, it can be seen that the active power loss and voltage deviation are in a downward trend with the increase of access number of SCs. The active power loss decreased from 151.38 KW to 141.72 KW, and the voltage deviation decreased from 0.0838 (p.u.) to 0.0633 (p.u.). It is not difficult to find that the active power losses reduced by three SCs are less than the active power losses reduced by one DG. This reflects that although the access of SC has a positive impact on improving the distribution network, it is less effective in improving the distribution network compared to DG.

In addition, it can be seen from this table that the optimization results of three DGs and SCs combinations are better than the previous six combinations. Under the combination of one DG and one SC, the transmission line loss of the system is only 58.45 KW, the other target value is also improved to 0.0173 (p.u.), which is more remarkable than that of three DGs. Finally, compared with other published research results, ISCSO algorithm is more effective in solving OARDN problem.

In Fig. 3, the node voltage curves of these nine combinations and the node voltage curves of the initial state are shown, which shows that the node voltage improvement is smaller for the three SCs combinations and the node voltage improvement is the largest for the three DGs and SCs combinations.

The optimization results of the second configuration scheme are shown in TABLE IV. It can be concluded from the table that, in the same combination configuration of DG and SC, P_{loss} and CV_d of the combination with a power factor of 0.9 are smaller than those of the combination with a power factor of 1. For example, when the power factor is 0.9, the P_{loss} of one DG is 70.86 KW, the CV_d is 0.0172 (p.u.), the P_{loss} of three DGs and SCs is 16.93 KW, CV_d is 0.0012 (p.u.). While when the power factor is 1, the P_{loss} of one DG is 111.03 KW, the CV_d is 0.0377 (p.u.), the P_{loss} of three DGs and SCs is 23.73 KW, CV_d is 0.0017 (p.u.). The result show a clear comparison. Fig. 4 shows the node voltage curves of several different combinations under the second configuration scheme. Similarly, the node voltage quality of the combination of three DGs and SCs is better.

2) Case2

In Case2, a single-objective experiment of OARDN problem will be conducted on IEEE69 test system. The test system has an initial transmission line loss of 226.64 KW and a voltage deviation of 0.0995 (p.u.). In this case, its configuration scheme is similar to Case1, which is also

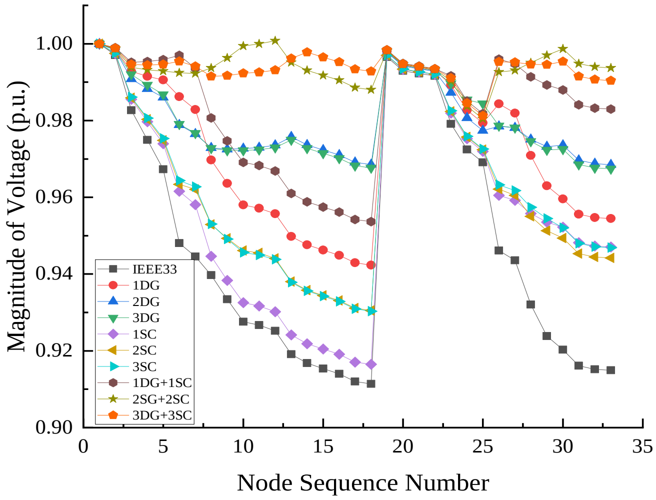

Fig. 3. Node voltage profile for the first type of configuration on IEEE33

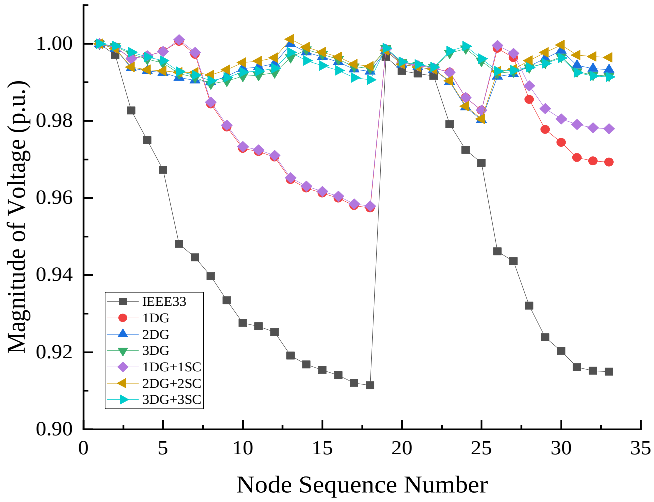

Fig. 4. Node voltage profile for the second type of configuration on IEEE33

TABLE V
THE FIRST TYPE OF CONFIGURATION SCHEME AND COMPARISON RESULTS FOR CASE2 (PF=1)

Configuration	Algorithms	Capacity (Location) of DGs	Capacity (Location) of SCs	P_{loss} (KW)	Percentage of original P_{loss} reduction	CV_d (p.u.)
	Case69			226.64		0.0995
1DG	ISCSO	1876.09(61)	-	83.92	62.97%	0.0208
2DG	ISCSO	532.56(18) 1783.71(61)	-	72.29	68.10%	0.0065
3DG	ISCSO	543.08(12) 251.58(22) 1741.20(61)	-	70.27	68.99%	0.0061
	IRRO [17]	784(12) 863(50) 1780(61)	-	71.14	68.61%	-
	PSO [17]	100(6) 100(41) 2000(61)	-	83.33	63.23%	-
	TLBO [41]	591.9(15) 818.8(61) 900.3(63)	-	72.41	68.05%	-
	LSFSA [36]	420.4(18) 1331.1(60) 429.8(65)	-	77.10	65.98%	-
1SC	ISCSO	-	1380.09(61)	153.23	32.35	0.0643
2SC	ISCSO	-	405.08(17) 1077.84(61)	149.03	34.24%	0.0618
3SC	ISCSO	-	326.50(16) 718.56(61) 617.50(62)	147.78	34.80%	0.0579
	COA [42]	-	300(17) 1500(57) 1208(61)	146.26	35.47%	-
1DG+1SC	ISCSO	1831.37(61)	1303.52(61)	23.49	89.64%	0.0121
2DG+2SC	ISCSO	857.67(12) 1703.20(61)	678.79(10) 1077.84(61)	9.91	95.63%	0.0016
3SG+3SC	ISCSO	308.77(10) 309.62(24) 1728.03(61)	718.56(61) 447.09(64) 389.41(68)	8.23	96.37%	0.0012

TABLE VI
The Second Type of Configuration Scheme for Case2 (PF=0.9)

Configuration	Algorithms	Capacity (Location) of DGs	Capacity (Location) of SCs	P_{loss} (KW)	Percentage of original P_{loss} reduction	CV_d (p.u.)
	Case69			226.64		0.0995
1DG	ISCSO	1999.27(61)	-	28.31	87.51%	0.0123
2DG	ISCSO	564.51(17) 1897.65(61)	-	12.51	94.48%	0.0005
3DG	ISCSO	436.89(17) 1842.98(61) 449.29(66)	-	9.92	95.62%	0.0001
1DG+1SC	ISCSO	1954.77(61)	638.18(12)	21.42	90.55%	0.0085
2DG+2SC	ISCSO	533.08(17) 1744.58(61)	330.02(64) 320.58(66)	6.36	97.19	0.0003
3SG+3SC	ISCSO	455.49(16) 1790.87(61) 192.41(69)	173.46(10) 66.82(36) 174.87(64)	6.57	97.10	0.0003

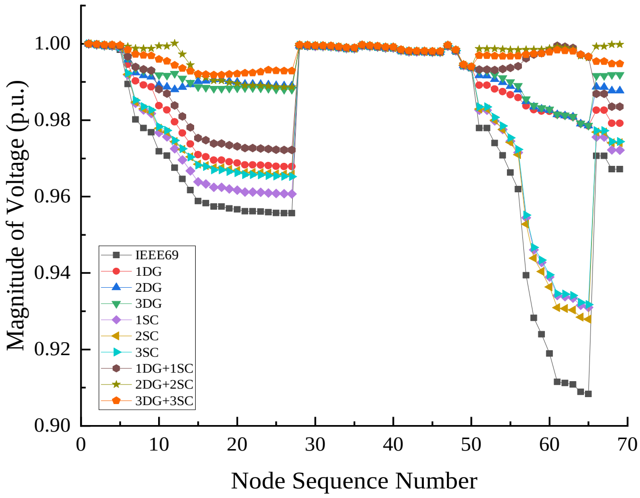
Fig. 5. Node voltage profile for the first type of configuration on IEEE69

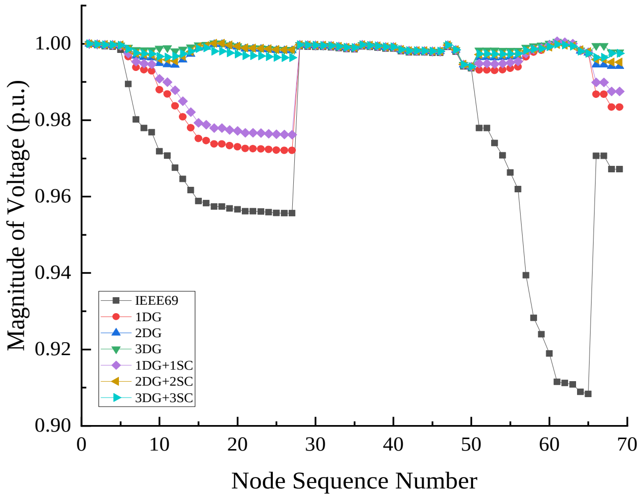
Fig. 6. Node voltage profile for the second type of configuration on IEEE69

divided into two types.

TABLE V shows the reduction of two types of target values achieved in the first type of configuration. The P_{loss} is 83.92 KW for a single DG, which is 62.97% lower than the initial P_{loss}, and 68.99% lower for three DGs, which is not a significant decrease. It can be inferred that increasing the number of DGs can make the active loss and voltage deviation in the system decrease further, but the magnitude of the decrease is not large, and blindly increasing the number of DGs makes the economic cost increase.

When three SCs are configured, it can be found that the P_{loss} value is 147.78 KW, with a decrease of only 34.8%, which further shows that the configuration of SC has less positive impact on the system than DG.

When the combination of DG and SC is deployed, the P_{loss} of just one DG and one SC is 23.49 KW, with a decrease of 89.64%, which is better than the results of the previous six configurations. The result of the configuration combination of two DGs and SCs is almost the same as that of three DGs and SCs, with a decrease of 95.63% and 96.37%, respectively. Such an optimization result is already satisfactory, so there is not much point in continuing to increase the number of devices.

Simultaneously, the comparison with other references is shown in the table. It can be seen that the proposed ISCSO algorithm is superior to most other existing methods, with only a small gap in some configuration combinations.

Fig. 5 shows the node voltage profiles for the nine configurations. It can be seen that the combined configuration of DG and SC is more effective for uniform voltage distribution.

The second configuration scheme of Case2 is consistent with that of Case1. When the power factor is 0.9, the P_{loss} under the configuration of 3 DGs is 9.92 KW, with a drop of 95.62%. Such a decrease is very significant and reflects the great influence of power factor. In TABLE VI, we find that the difference between the three DGs configurations and the combined deployment of three electrical devices is not significant, but in Fig. 6, we can find that there is a remarkable difference in the node voltage distribution between these two configurations, the node voltage distribution of DGs and SCs configuration is more uniform and less volatile.

3) Case3

This case will be tested on IEEE119 test system, and it is also divided into two types of configuration schemes. Compared with the IEEE33 and IEEE69 systems, this test system is much larger in size and therefore has a larger amount of data, which is more testing and challenging for the proposed ISCSO algorithm to solve the single objective problem of OARDN. In TABLE VII, it can be seen that due to the expansion of the system scale, the line loss of the initial system is larger, and the value of P_{loss} reaches 978.08 KW. Under different combination configurations, it can be seen that the reduction of power loss is not significant, the maximum value is only 59.6%, however, the power loss is reduced by 582.85 KW, such an optimization result is very significant. Similar to the trend in the previous two cases, as

TABLE VII
THE FIRST TYPE OF CONFIGURATION SCHEME FOR CASE3 (PF=1)

Configuration	Algorithms	Capacity (Location) of DGs	Capacity (Location) of SCs	P_{loss} (KW)	Percentage of original P_{loss} reduction	CV_d (p.u.)
	Case119			978.08		0.1875
1DG	ISCSO	2846.13(111)	-	828.53	15.29%	0.1557
2DG	ISCSO	3592.53(68) 2846.81(111)	-	686.41	29.82%	0.1113
3DG	ISCSO	2903.56(39) 3321.33(68) 2868.02(111)	-	571.01	41.62%	0.0831
1SC	ISCSO	-	2326.81(111)	875.525	10.49%	0.1706
2SC	ISCSO	-	2592.66(38) 2326.62(111)	809.33	17.25%	0.1429
3SC	ISCSO	-	2571.70(38) 2222.03(68) 2350.66(111)	748.09	23.51%	0.1211
1DG+1SC	ISCSO	3589.81(68)	2327.55(111)	733.40	25.02%	0.1263
2DG+2SC	ISCSO	2755.67(40) 3028.64(110)	2510.12(68) 2415.74(111)	561.51	42.59%	0.0973
3SG+3SC	ISCSO	3901.68(37) 2217.45(70) 3320.52(110)	2608.66(35) 1569.33(82) 1709.18(112)	395.23	59.60%	0.0537

TABLE VIII
THE SECOND TYPE OF CONFIGURATION SCHEME FOR CASE3 (PF=0.9)

Configuration	Algorithms	Capacity (Location) of DGs	Capacity (Location) of SCs	P_{loss} (KW)	Percentage of original P_{loss} reduction	CV_d (p.u.)
	Case119			978.08		0.1875
1DG	ISCSO	3183.71(111)	-	749.42	23.38%	0.1519
2DG	ISCSO	3810.30(68) 3182.76(111)	-	554.00	43.36%	0.0974
3DG	ISCSO	3837.58(38) 3729.19(68) 3039.58(111)	-	380.96	61.05%	0.0551
1DG+1SC	ISCSO	3810.34(68)	2327.11(111)	680.09	30.47%	0.1161
2DG+2SC	ISCSO	3840.28(38) 3264.90(111)	1204.78(51) 1505.48(68)	467.55	52.20%	0.0854
3SG+3SC	ISCSO	3267.85(39) 3508.96(68) 3365.76(111)	1040.11(24) 1339.02(51) 453.62(87)	299.53	69.38%	0.3936

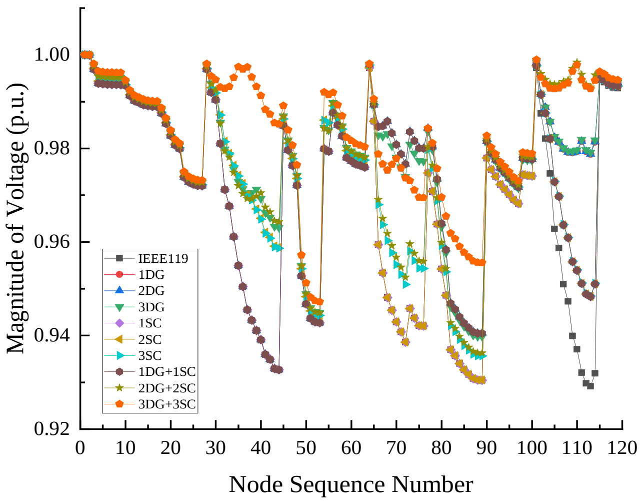

Fig. 7. Node voltage profile for the first type of configuration on IEEE119

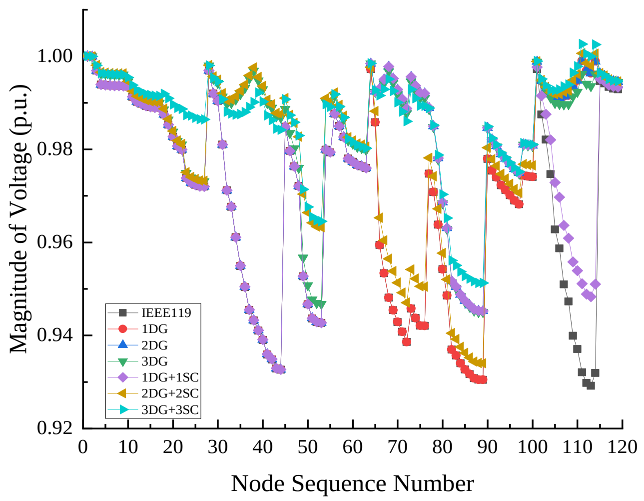

Fig. 8. Node voltage profile for the second type of configuration on IEEE119

the equipment quantity increases, the energy waste and voltage deviation decrease, but the difference is that in this case, three independently configured DGs or three jointly configured DGs and SCs are not the optimal solution, and the number of devices can continue to increase as needed to further achieve the active loss or voltage deviation reduction. In Fig. 7, it can be seen that the voltage fluctuations at each node are larger for different configuration schemes, but the node voltage distribution is more uniform for the three jointly configured DGs and SCs.

TABLE VIII lists the second configuration scheme (PF=0.9) and the results. The data in this table further shows that the difference of power factor does affect the power loss and voltage deviation. It can be seen from Fig. 8 that the configuration combination with SC has better node voltage distribution and smaller voltage fluctuation than the configuration combination without SC.

B. Multi Objective Simulation for OARDN

In the multi-objective research, it is difficult to obtain an excellent Pareto frontier only by solving the optimal configuration of DG and SC by optimization algorithm, so this study proposes a method for sensitivity analysis. The approach aims to access a DG or SC unit with a very small capacity at one node of the system and observe the impact degree on the whole system. The sensitivity values at each node are calculated by equations (28) and (29).

$$SenDG_i = \frac{P_{loss} - P_{loss(i)}}{\Delta P_{DG}} \tag{28}$$

$$SenSC_i = \frac{P_{loss} - P_{loss(i)}}{\Delta Q_{SC}} \tag{29}$$

Among them, DG_i and SC_i represent DG or SC connected by the ith node, P_{loss} represents the active power loss of the standard system, and $P_{loss(i)}$ represents the active power loss of the system after the ith node is connected to DG or SC. According to the calculated sensitivity value, the node with larger sensitivity value is selected as the best access location of DG or SC. Fig. 9, Fig. 10 and Fig. 11 show the sensitivity values of DG and SC of each node under three standard test systems.

1) Case4

By introducing the sensitivity analysis method, multi-objective constraint processing strategy and pareto non-inferior sorting method into the ISCSO algorithm, a MOISCSO algorithm for solving the multi-objective OARDN problem is formed.

In this case, the MOISCSO algorithm and MOSCSO algorithm will be used to find a set of DG and SC configuration schemes that makes the P_{loss} and CV_d smaller under the IEEE33 test system. Fig. 12 shows the Pareto fronts (PFs) of the two algorithms for the configuration scheme of

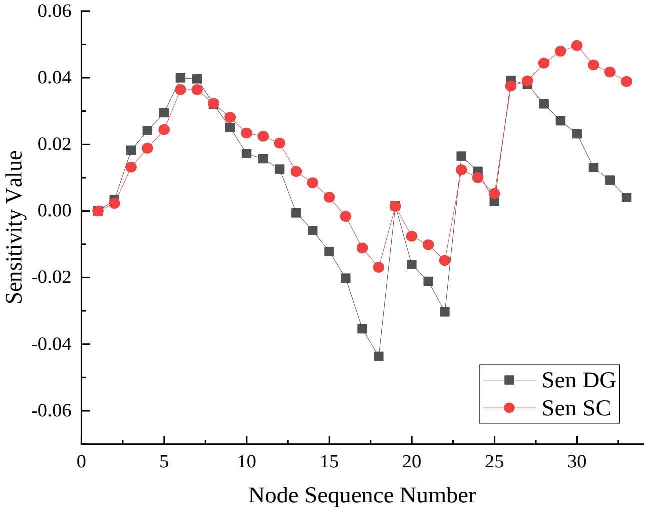

Fig. 9.Sensitivity values of DG and SC on IEEE33 test system

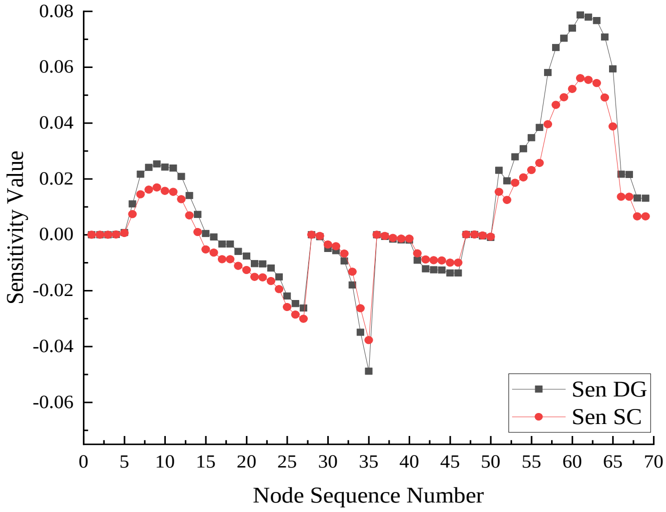

Fig. 10. Sensitivity values of DG and SC on IEEE69 test system

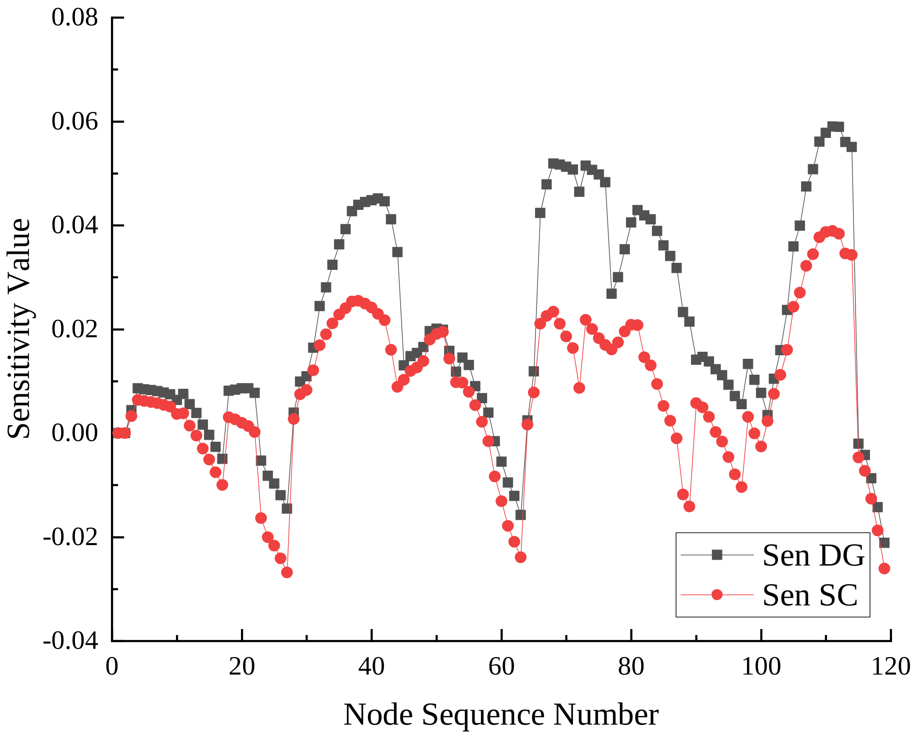

Fig. 11. Sensitivity values of DG and SC on IEEE119 test system

one DG and one SC. The minimum values of P_{loss} and CV_d as well as the best compromise solution (BCS) are marked in the figure. From the data in TABLE IX, it can be found that the BCS solution of the MOISCSO algorithm is 59.77 KW, 0.0052 (p.u.), which is better than the BCS of the MOSCSO algorithm, indicating that the PFs of the MOISCSO algorithm is near to the true PF. The two-device deployment scheme's PFs and improved results are displayed in Fig. 13 and TABLE X. Similarly, the BCS of MOISCSO algorithm is better than that of MOSCSO algorithm. It further shows that MOISCSO algorithm is more advantageous than MOSCSO algorithm, and it is more competitive in dealing with multi-objective OARDN problems.

2) Case5

Under the IEEE69 test system, like Case 4, the multi-objective OARDN problem of two types of combination configuration is studied. The PFs and the values of BCS for the MOISCSO and MOSCSO algorithms are given in Fig. 14 and TABLE XI. As can be clearly seen, the Pareto solution set of MOISCSO is more uniform, while on the contrary, the Pareto solution set of MOSCSO is more scattered and even has breakpoints.

Fig. 15 and TABLE XII then give the values of PF and BCS for the configuration scheme with two DGs and two SCs. Their BCS values are 13.08 KW and 0.0014 (p.u.), respectively, and the BCS of this configuration scheme is significantly better than the BCS of the configuration combination of one DG and SC.

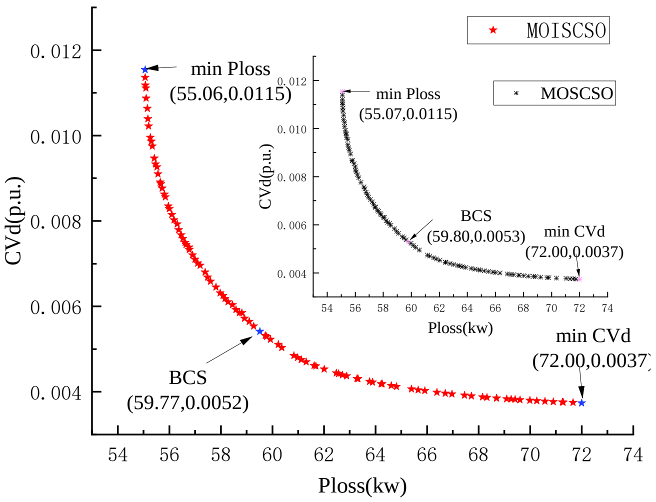

Fig. 12.PFs of MOISCSO algorithm and MOSCSO algorithm on IEEE33 (1DG+1SC)

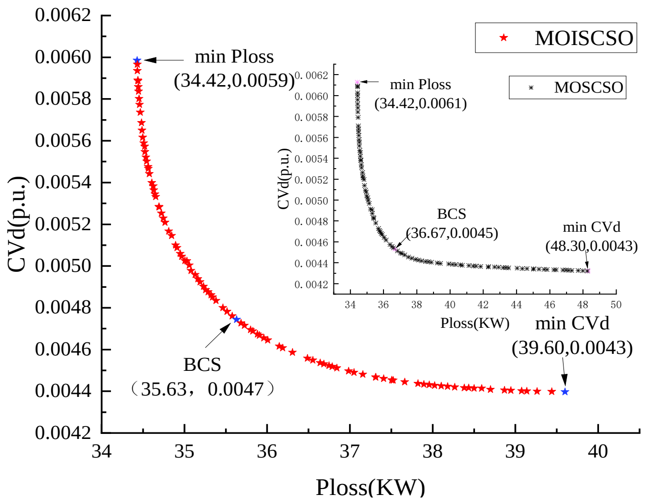

Fig. 13. PFs of MOISCSO algorithm and MOSCSO algorithm on IEEE33 (2DG+2SC)

TABLE IX
1DG+1SC configuration scheme on IEEE33

Configuration	Algorithms	BCS f_{Ploss}	BCS f_{CVd}	Min P_{loss} f_{Ploss}	Min P_{loss} f_{CVd}	Min CVd f_{Ploss}	Min CVd f_{CVd}
1DG+1SC	MOISCSO	59.77	0.0052	55.06	0.0115	72.00	0.0037
	Capacity (Location) of DGs	29179.11(7)		2403.32(7)		2972(7)	
	Capacity (Location) of SCs	1503.25(30)		1327.15(30)		1976(30)	
	MOSCSO	59.80	0.0053	55.07	0.0115	72.00	0.0037
	Capacity (Location) of DGs	2926.51(7)		2403.42(7)		2972(7)	
	Capacity (Location) of SCs	1492.97(30)		1328.01(30)		1.976(30)	

TABLE X
2DG+2SC configuration scheme on IEEE33

Configuration	Algorithms	BCS f_{Ploss}	BCS f_{CVd}	Min P_{loss} f_{Ploss}	Min P_{loss} f_{CVd}	Min CVd f_{Ploss}	Min CVd f_{CVd}
2DG+2SC	MOISCSO	35.63	0.0047	34.42	0.0059	39.60	0.0043
	Capacity (Location) of DGs	1486(7) 1041.56(7)		1486(7) 876.21(7)		1486(7) 1279.93(7)	
	Capacity (Location) of SCs	988(30) 988(30)		962.64(30) 907.65(30)		988(30) 940.39(30)	
	MOSCSO	36.67	0.0045	34.42	0.0061	48.30	0.0043
	Capacity (Location) of DGs	1486(7) 1122.50(30)		1486(7) 866.68(30)		1486(7) 1486(30)	
	Capacity (Location) of SCs	988(7) 988(30)		950.22(7) 907.94(30)		988(7) 618.75(30)	

3) Case6

Similarly, testing on a large test system provides a more comprehensive evaluation of the proposed method. Therefore, this case will solve the multi-objective OARDN problem of two configuration schemes on IEEE119 test system. Fig. 16 presents the Pareto fronts obtained by optimizing both P_{loss} and CV_d for one DG and SC configuration. The values of the BCS are given in TABLE XIII with a P_{loss} of 1003.47 KW and a CV_d of 0.1191 (p.u.).

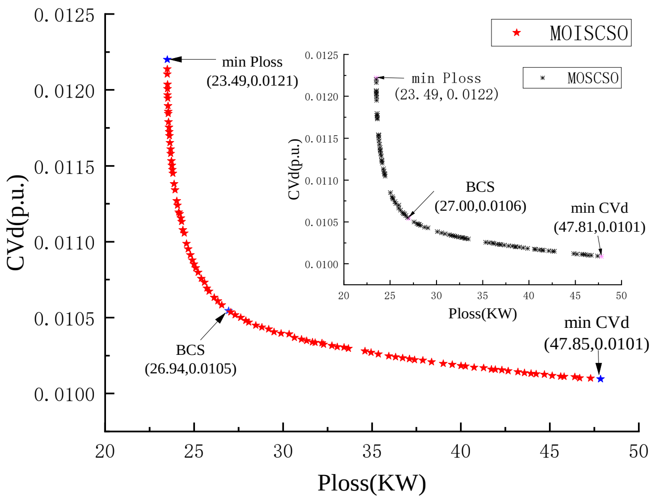

Fig. 14. PFs of MOISCSO algorithm and MOSCSO algorithm on IEEE69 (1DG+1SC)

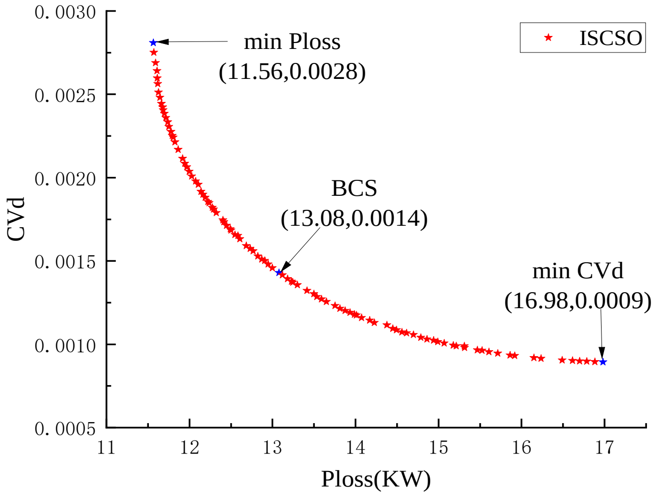

Fig. 15. PFs of MOISCSO algorithm on IEEE69 (2DG+2SC)

TABLE XI
1DG+1SC configuration scheme on IEEE69

Configuration	Algorithms	BCS f_{Ploss}	BCS f_{CVd}	Min P_{loss} f_{Ploss}	Min P_{loss} f_{CVd}	Min CVd f_{Ploss}	Min CVd f_{CVd}
1DG+1SC	MOISCSO	26.94	0.0105	23.49	0.0121	47.85	0.0101
	Capacity (Location) of DGs	2065.48(61)		1830.62(61)		1905.25(61)	
	Capacity (Location) of SCs	1527.71(61)		1302.91(61)		2155.68(61)	
	MOSCSO	27.00	0.0106	23.49	0.0122	47.81	0.0101
	Capacity (Location) of DGs	2058.77(61)		1829.86(61)		1877.04(61)	
	Capacity (Location) of SCs	1537.66(61)		1299.17(61)		2155.68(61)	

TABLE XII
2DG+2SC configuration scheme on IEEE69

Configuration	Algorithms	BCS f_{Ploss}	BCS f_{CVd}	Min P_{loss} f_{Ploss}	Min P_{loss} f_{CVd}	Min CVd f_{Ploss}	Min CVd f_{CVd}
2DG+2SC	MOISCSO	13.08	0.0014	11.56	0.0028	16.98	0.0009
	Capacity (Location) of DGs	1295.25(11) 1516.76(61)		1053.24(11) 1516.76(61)		1516.76(11) 1516.76(61)	
	Capacity (Location) of SCs	833.55(11) 1077.84(61)		638.47(11) 1077.84(61)		1077.84(11) 1077.84(61)	

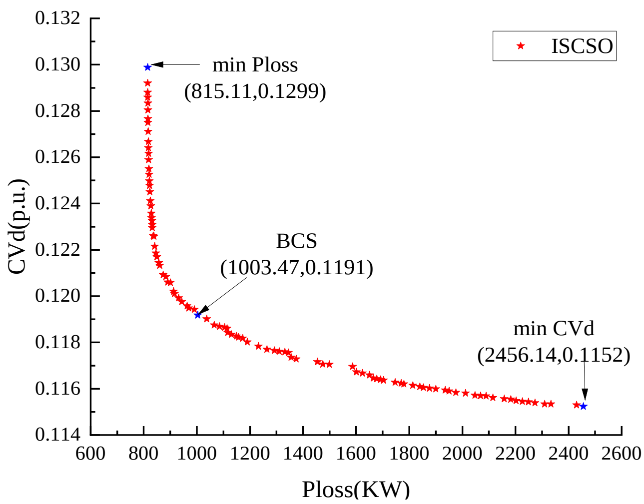

Fig. 16. PFs of MOISCSO algorithm on IEEE119 (1DG+1SC)

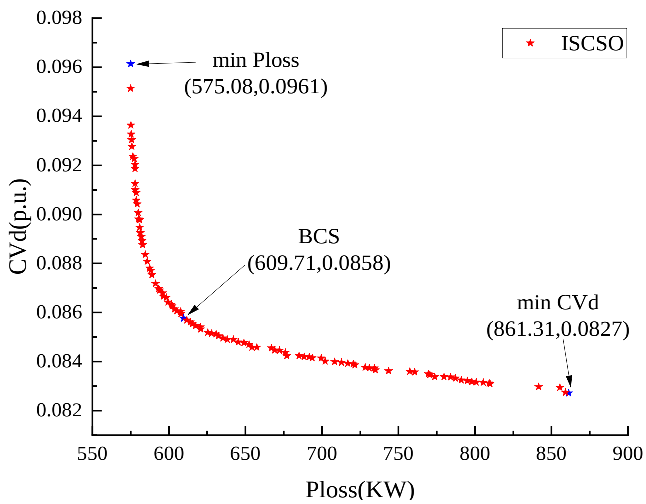

Fig. 17. PFs of MOISCSO algorithm on IEEE119(2DG+2SC)

TABLE XIII
1DG+1SC configuration scheme on IEEE119

Configuration	Algorithms	BCS		Min Ploss		Min CVd	
		f_{Ploss}	f_{CVd}	f_{Ploss}	f_{CVd}	f_{Ploss}	f_{CVd}
1DG+1SC	MOISCSO	1003.47	0.1191	815.11	0.1299	2456.14	0.1152
	Capacity (Location) of DGs	2956.35(111)		2883.43(111)		0(111)	
	Capacity (Location) of SCs	6124.11(111)		2078.69(111)		13632.85(111)	

TABLE XIV
2DG+2SC configuration scheme on IEEE119

Configuration	Algorithms	BCS		Min Ploss		Min CVd	
		f_{Ploss}	f_{CVd}	f_{Ploss}	f_{CVd}	f_{Ploss}	f_{CVd}
2DG+2SC	MOISCSO	609.71	0.0858	575.08	0.0961	861.31	0.0827
	Capacity (Location) of DGs	3986.29(81)		2607.64(81)		2795.16(81)	
		3048.1(111)		2823.99(111)		2514.65(111)	
	Capacity (Location) of SCs	3425.83(81)		2057.31(81)		6816.43(81)	
		2508.86(111)		2407.09(111)		3626.64(111)	

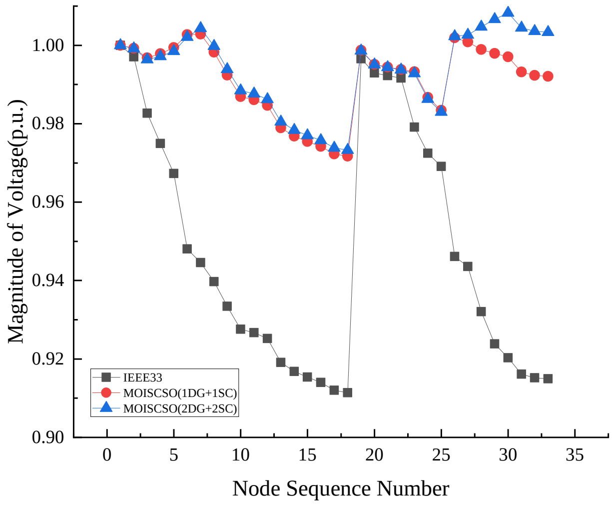

Fig. 18. Node voltage profile of BCS of MOISCSO on IEEE33

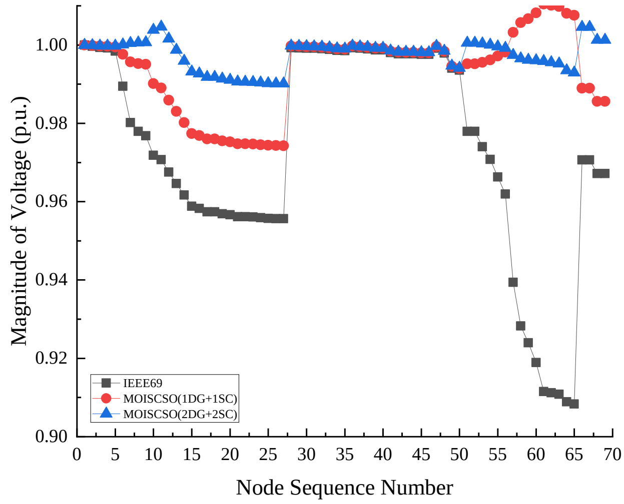

Fig. 19. Node voltage profile of BCS of MOISCSO on IEEE69

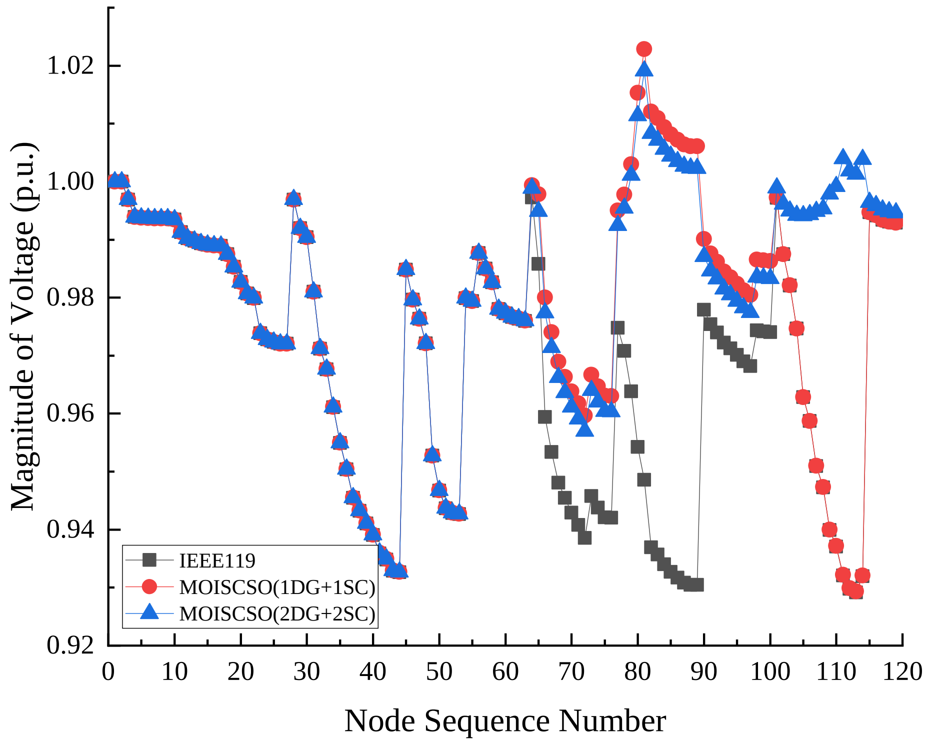

Fig. 20. Node voltage profile of BCS of MOISCSO on IEEE119

Fig. 17 shows the PF for the configuration with two DGs and SCs, while TABLE XIV presents the data results. It can be seen from the figure that there is a discontinuity at both ends of PF, but overall, the quality of solution set is not affected. The values of the BCS are 609.71 KW and 0.0858 (p.u.), respectively.

This case also verifies that the MOISCSO algorithm is extremely practical for solving multi-objective OARDN problems.

In Fig. 18, Fig. 19 and Fig. 20, the node voltage profile of BCS of MOISCSO algorithm in three different test systems is shown. It can be seen that the voltage distribution curve obtained by MOISCSO is better than the initial node voltage profile. Although the voltage of some nodes is a little high, it is also within the reasonable range of voltage constraints.

V. CONCLUSION

This study focuses on addressing the limitations of SCSO algorithm, which are primarily attributed to its susceptibility to local optima and suboptimal convergence, three improvement measures are introduced, namely tent chaotic mapping mechanism, reverse learning strategy and cross learning mechanism, and ISCSO algorithm is proposed in combination with single-objective constraint processing strategy. At the same time, considering the lack of multi-objective research on OARDN, to expand the ability of the proposed method to solve OARDN problems, this paper introduces the proposed multi-objective constraint processing strategy, sensitivity analysis method and pareto non-inferior sorting method into ISCSO algorithm, and forms MOISCSO algorithm to deal with multi-objective OARDN problems.

In order to study the practicality and advantages of ISCSO algorithm and MOISCSO algorithm, simulation experiments of single-objective and multi-objective OARDN issues were conducted in three different scale test systems. The results of single-objective optimization show that one single DG access can significantly reduce the power loss and voltage deviation in the system. With the increase in the number of DG devices, the reduction range of the objective value is obviously reduced. The access of SC is not as effective as DG in optimizing the two objective functions, but it has a significant effect on improving the voltage of each node in the system. The combination of DG and SC is the most effective for reducing power loss and voltage deviation. The multi-objective optimization outcomes demonstrate the proposed approach can tackle the multi-objective OARDN problem and yield a set of well-distributed pareto solutions. Compared with the MOSCSO algorithm, it can also be found that the Pareto solution set of MOISCSO algorithm is closer to the real pareto frontier.

In conclusion, the ISCSO and MOISCSO algorithms proposed in this paper provide a better solution to get the best configuration scheme for the OARDN problem, which is more helpful for the safe and stable operation of the distribution network.

REFERENCES

[1] A. M. Shaheen, A. M. Elsayed, A. R. Ginidi, R. A. El-Sehiemy and E. Elattar, "A heap-based algorithm with deeper exploitative feature for optimal allocations of distributed generations with feeder reconfiguration in power distribution networks," Knowledge-Based Systems, vol. 241, article. 108269, 2022.

[2] A. M. Elsayed, M. M. Mishref and S. M. Farrag, "Distribution system performance enhancement (Egyptian distribution system real case study)," International Transactions on Electrical Energy Systems, vol. 28, no. 6, article. e2545, 2018.

[3] T. E. Gümüş, S. Emiroglu and M. A. Yalcin, "Optimal DG allocation and sizing in distribution systems with Thevenin based impedance stability index," International Journal of Electrical Power & Energy Systems, vol. 144, article. 108555, 2023.

[4] A. Noori, Y. Zhang, N. Nouri and M. Hajivand, "Hybrid allocation of capacitor and distributed static compensator in radial distribution networks using multi-objective improved golden ratio optimization based on fuzzy decision making," IEEE Access, vol. 8, pp. 162180-162195, 2020.

[5] V. Tamilselvan, T. Jayabarathi, T. Raghunathan and X. Yang, "Optimal capacitor placement in radial distribution systems using flower pollination algorithm," Alexandria Engineering Journal, vol. 57, no. 4, pp. 2775-2786, 2018.

[6] A. Askarzadeh, "Capacitor placement in distribution systems for power loss reduction and voltage improvement: A new methodology," IET Generation, Transmission & Distribution, vol. 10, no. 14, pp. 3631-3638, 2016.

[7] T. P. Nguyen, T. A. Nguyen, T. V. Phan and D. N. Vo, "A comprehensive analysis for multi-objective distributed generations and capacitor banks placement in radial distribution networks using hybrid neural network algorithm," Knowledge-Based Systems, vol. 231, article. 107387, 2021.

[8] A. M. Shaheen, A. M. Elsayed, R. A. El-Sehiemy and A. Y. Abdelaziz, "Equilibrium optimization algorithm for network reconfiguration and distributed generation allocation in power systems," Applied Soft Computing, vol. 98, article. 106867, 2021.

[9] R. Palanisamy and S. K. Muthusamy, "Optimal siting and sizing of multiple distributed generation units in radial distribution system using ant lion optimization algorithm," Journal of Electrical Engineering & Technology, vol. 16, no. 1, pp. 79-89, 2021.

[10] A. S. Hassan, Y. Sun and Z. Wang, "Multi-objective for optimal placement and sizing DG units in reducing loss of power and enhancing voltage profile using BPSO-SLFA," Energy Reports, vol. 6, pp. 1581-1589, 2020.

[11] E. A. Almabsout, R. A. El-Sehiemy, O. N. U. An and O. Bayat, "A hybrid local Search-Genetic algorithm for simultaneous placement of DG units and shunt capacitors in radial distribution systems," IEEE Access, vol. 8, pp. 54465-54481, 2020.

[12] A. Verma and R. Thakur, "A review on methods for optimal placement of distributed generation in distribution network," in 2022 Interdisciplinary Research in Technology and Management (IRTM), 2022, pp. 1-8.

[13] Y. Li, B. Feng, B. Wang and S. Sun, "Joint planning of distributed generations and energy storage in active distribution networks: A Bi-Level programming approach," Energy, vol. 245, article. 123226, 2022.

[14] K. H. Truong, P. Nallagownden, I. Elamvazuthi and D. N. Vo, "A Quasi-Oppositional-Chaotic Symbiotic Organisms Search algorithm for optimal allocation of DG in radial distribution networks," Applied Soft Computing, vol. 88, article. 106067, 2020.

[15] M. Inoue, T. Sadamoto, M. Arahata and A. Chakrabortty, "Optimal power flow design for enhancing dynamic performance: Potentials of reactive power," IEEE Transactions On Smart Grid, vol. 12, no. 1, pp. 599-611, 2021.

[16] C. Zhang, Q. Liu, S. Huang, B. Zhou and L. Cheng et al., "Reactive power optimization under interval uncertainty of renewable power generation based on a security limits method," International Journal of Electrical Power & Energy Systems, vol. 130, article. 106894, 2021.

[17] M. K. Mangoli, K. Y. Lee and Y. Moon Park, "Optimal real and reactive power control using linear programming," Electric Power Systems Research, vol. 26, no. 1, pp. 1-10, 1993.

[18] M. M. Aman, G. B. Jasmon, H. Mokhlis and A. H. A. Bakar, "Optimum tie switches allocation and DG placement based on maximisation of system loadability using discrete artificial bee colony algorithm," IET Generation, Transmission & Distribution, vol. 10, no. 10, pp. 2277-2284, 2016.

[19] H. Manafi, N. Ghadimi, M. Ojaroudi and P. Farhadi, "Optimal placement of distributed generations in radial distribution systems using various PSO and DE algorithms," Electronics and Electrical Engineering, vol. 19, no. 10, 2013.

[20] N. H. Awad, M. Z. Ali, R. Mallipeddi and P. N. Suganthan, "An Efficient Differential Evolution Algorithm for Stochastic OPF based Active-Reactive Power Dispatch Problem considering Renewable Generators," Applied Soft Computing, vol. 76, pp. 445-458, 2019.

[21] M. M. Aman, G. B. Jasmon, A. H. A. Bakar and H. Mokhlis, "A new approach for optimum simultaneous multi-DG distributed generation Units placement and sizing based on maximization of system loadability using HPSO (hybrid particle swarm optimization) algorithm," Energy, vol. 66, pp. 202-215, 2014.
[22] A. Y. Abdelaziz, R. A. Osama, S.M. El-Khodary, "Reconfiguration of distribution systems for loss reduction using the hyper-cube ant colony optimisation algorithm," IET Generation, Transmission & Distribution, pp. 79-84, 2011.
[23] S. Nagaballi and V. S. Kale, "Pareto optimality and game theory approach for optimal deployment of DG in radial distribution system to improve techno-economic benefits," Applied Soft Computing, vol. 92, article. 106234, 2020.
[24] K. H. Truong, P. Nallagownden, I. Elamvazuthi and D. N. Vo "A Quasi-Oppositional-Chaotic symbiotic organisms search algorithm for optimal allocation of DG in radial distribution networks," Applied Soft Computing Journal, vol. 88, article. 106067, 2020.
[25] M. Purlu and B. E. Turkay, "Optimal allocation of renewable distributed generations using heuristic methods to minimize annual energy losses and voltage deviation index," IEEE Access, vol. 10, pp. 21455-21474, 2022.
[26] A. Arasteh, P. Alemi and M. Beiraghi, "Optimal allocation of photovoltaic/wind energy system in distribution network using meta-heuristic algorithm," Applied Soft Computing, vol. 109, article. 107594, 2021.
[27] M. R. Elkadeem, M. Abd Elaziz, Z. Ullah, S. Wang and S. W. Sharshir, "Optimal planning of renewable Energy-Integrated distribution system considering uncertainties," IEEE Access, vol. 7, pp. 164887-164907, 2019.
[28] T. S. Tawfeek, A. H. Ahmed and S. Hasan, "Analytical and particle swarm optimization algorithms for optimal allocation of four different distributed generation types in radial distribution networks," Energy Procedia, vol. 153, pp. 86-94, 2018.
[29] D. Q. Hung and N. Mithulananthan, "Multiple distributed generator placement in primary distribution networks for loss reduction," IEEE Transactions on Industrial Electronics, vol. 60, no. 4, pp. 1700-1708, 2013.
[30] T. P. Nguyen, T. A. Nguyen, T. V. Phan and D. N. Vo, "A comprehensive analysis for multi-objective distributed generations and capacitor banks placement in radial distribution networks using hybrid neural network algorithm," Knowledge-Based Systems, vol. 231, article. 107387, 2021.
[31] K. Mahmoud, N. Yorino and A. Ahmed, "Optimal distributed generation allocation in distribution systems for loss minimization," IEEE Transactions on Power Systems, vol. 31, no. 2, pp. 960-969, 2016.
[32] H. Long, Y. He and Y. HE, "Application of improved honey badger algorithm in multi-objective reactive power optimization," IAENG International Journal of Applied Mathematics, vol. 52, no. 4, pp. 1105-1122, 2022.
[33] A. Seyyedabbasi and F. Kiani, "Sand Cat swarm optimization: A nature-inspired algorithm to solve global optimization problems," Engineering with Computers, 2022.
[34] A. El-Fergany, "Optimal allocation of multi-type distributed generators using backtracking search optimization algorithm," International Journal of Electrical Power & Energy Systems, vol. 64, pp. 1197-1205, 2015.
[35] R. Palanisamy and S. K. Muthusamy, "Optimal siting and sizing of multiple distributed generation units in radial distribution system using ant lion optimization algorithm," Journal of Electrical Engineering & Technology, vol. 16, no. 1, pp. 79-89, 2021.
[36] S. K. Injeti and N. Prema Kumar, "A novel approach to identify optimal access point and capacity of multiple DGs in a small, medium and large scale radial distribution systems," International Journal of Electrical Power & Energy Systems, vol. 45, no. 1, pp. 142-151, 2013.
[37] M. H. Moradi and M. Abedini, "A novel method for optimal DG units capacity and location in Microgrids," International Journal of Electrical Power & Energy Systems, vol. 75, pp. 236-244, 2016.
[38] D. B. Prakash and C. Lakshminarayana, "Multiple DG placements in radial distribution system for multi objectives using Whale Optimization Algorithm," Alexandria Engineering Journal, vol. 57, no. 4, pp. 2797-2806, 2018.
[39] A. Khodabakhshian and M. H. Andishgar, "Simultaneous placement and sizing of DGs and shunt capacitors in distribution systems by using IMDE algorithm," International Journal of Electrical Power & Energy Systems, vol. 82, pp. 599-607, 2016.
[40] M. Dixit, P. Kundu and H. R. Jariwala, "Incorporation of distributed generation and shunt capacitor in radial distribution system for techno-economic benefits," Engineering Science and Technology, an International Journal, vol. 20, no. 2, pp. 482-493, 2017.
[41] S. Sultana and P. K. Roy, "Multi-objective quasi-oppositional teaching learning based optimization for optimal location of distributed generator in radial distribution systems," International Journal of Electrical Power & Energy Systems, vol. 63, pp. 534-545, 2014.
[42] A. Youssef, S. Kamel, M. Ebeed and J. Yu, "Optimal capacitor allocation in radial distribution networks using a combined optimization approach," Electric Power Components and Systems, vol. 46, no. 19-20, pp. 2084-2102, 2018.